

Carbon monoxide interacting with free-electron-laser pulses

H. I. B. Banks

Department of Physics and Astronomy, University College London, Gower Street, London WC1E 6BT, United Kingdom

A. Hadjipittas

Department of Physics and Astronomy, University College London, Gower Street, London WC1E 6BT, United Kingdom

A. Emmanouilidou

Department of Physics and Astronomy, University College London, Gower Street, London WC1E 6BT, United Kingdom

Abstract. We study the interaction of a heteronuclear diatomic molecule, carbon monoxide, with a free-electron laser (FEL) pulse. We compute the ion yields and the intermediate states by which the ion yields are populated. We do so using rate equations, computing all relevant molecular and atomic photoionisation cross-sections and Auger rates. We find that the charge distribution of the carbon and oxygen ion yields differ. By varying the photon energy, we demonstrate how to control higher-charged states being populated mostly by carbon or oxygen. Moreover, we identify the differences in the resulting ion yields and pathways populating these yields between a homonuclear molecule, molecular nitrogen, and a heteronuclear molecule, carbon monoxide, interacting with an FEL pulse. These two molecules have similar electronic structure. We also identify the proportion of each ion yield which accesses a two-site double-core-hole state and tailor pulse parameters to maximise this proportion.

PACS numbers: 33.80.Rv, 34.80.Gs, 42.50.Hz

Submitted to: *J. Phys. B: At. Mol. Opt. Phys.*

1. Introduction

X-ray free-electron lasers (XFELs) [1–3] have introduced new tools and techniques for the investigation and imaging of atoms and molecules [4, 5]. The x-ray energy of the photons and high intensity of the FEL pulses allow for high-resolution images of large biomolecules [6–8]. These x-ray photons are also more likely to ionise inner-shell electrons than valence electrons, resulting in the creation of core holes. If another core hole is created, before the atom or molecule has time to relax via Auger processes, a double-core-hole (DCH) state is formed. In molecules, there are two types of DCH states, those where both core holes are on the same atomic site, i.e. single-site double-core-hole (SSDCH) states, and those where the core holes are on different atomic sites, i.e. two-site double-core-hole (TSDCH) states. These TSDCH states are particularly interesting due to their sensitivity to their chemical environment [9–13]. Double-core-hole states are short-lived, as they decay via Auger processes. This process involves a core hole being filled in by a valence electron, while the released energy results in the ejection of another valence electron. There has been a significant amount of both experimental [14–18] and theoretical [19, 20] work regarding these states.

We investigate the influence of two-site double-core-hole states during the interaction of an FEL pulse with a heteronuclear diatomic molecule. Specifically, we identify the set of pulse parameters that maximise the production of two-site double-core-hole states during the interaction of carbon monoxide (CO) with an FEL pulse. The interaction of CO with an FEL pulse has been the focus of several studies, as it pertains to biomolecules [21, 22]. The formation of TSDCH states in CO has been detected experimentally through photoelectron spectra [14], with supporting theoretical energy calculations [11]. In the current study, we investigate the effect of the photon energy, pulse duration and intensity of the pulse on the contribution of TSDCHs in the formation of the final ion yields. As a result, we identify the most appropriate FEL pulse parameters for maximising the proportion of the final ion yields that accesses a TSDCH. In addition, we investigate the role of TSDCH states during the interaction of an FEL pulse with a homonuclear versus a heteronuclear diatomic molecule. We do so in the context of molecular nitrogen (N_2) versus CO, two diatomic molecules of similar electronic structure.

Moreover, we investigate whether carbon or oxygen populate more highly-charged states during the interaction of CO with an FEL pulse. That is, by varying the photon energy as well as the duration and intensity of the FEL pulse we identify which pulse parameters favour higher-charged states being populated by carbon or oxygen. In addition, for the same FEL pulse parameters we compare the resulting carbon and oxygen ion yields with the atomic nitrogen yields resulting from the FEL pulses interacting with N_2 . This allows us to identify additional differences in the interaction of homonuclear and heteronuclear molecules with FEL pulses.

2. Method

2.1. Rate Equations

We use rate equations to model the interaction of FEL pulses with CO. Every energetically accessible state of CO is denoted by its electronic configuration, $(1\sigma^a, 2\sigma^b, 3\sigma^c, 4\sigma^d, 1\pi_x^e, 1\pi_y^f, 5\sigma^g)$, where a, b, c, d, e, f and g are the number of electrons occupying a molecular orbital. This occupancy is 0, 1 or 2. These rate equations were discussed in detail in previous work in the context of the homonuclear molecule N_2 $(1\sigma_g^a, 1\sigma_u^b, 2\sigma_g^c, 2\sigma_u^d, 1\pi_{ux}^e, 1\pi_{uy}^f, 3\sigma_g^g)$ interacting with FEL pulses [23]. In the rate equations describing the interaction of CO with an FEL pulse we employ the single-photon ionisation cross-section and Auger rates for all energetically allowed transitions in CO as well as its atomic fragments. Atomic units are used in this work, unless otherwise stated. To obtain these cross sections and rates we need to compute the bound and the continuum atomic and molecular orbitals for all energetically accessible states. To simplify the computations involved for the photoionisation cross-section and Auger rates, we express these orbitals in terms of a single-centre expansion (SCE) [24].

2.2. Bound and continuum orbitals

We obtain the molecular and atomic bound wavefunctions ψ_i using the Hartree-Fock technique in Molpro [25], a quantum chemistry package. We use the cc-pVTZ basis set to obtain the bound wavefunctions for CO with the nuclei fixed at an equilibrium distance of 1.128 Å [26]. In the single-centre expansion the bound and continuum wavefunctions, ψ_i and ψ_ϵ respectively, are expressed as [24]

$$\psi_{(i/\epsilon)}(\mathbf{r}) = \sum_{lm} \frac{P_{lm}^{i/\epsilon}(r) Y_{lm}(\theta, \phi)}{r}, \quad (1)$$

with $\mathbf{r} = (r, \theta, \phi)$ denoting the position of the electron, with respect to the centre of mass of the molecule. We denote by Y_{lm} , a spherical harmonic with quantum numbers l and m while $P_{lm}^{i/\epsilon}(r)$ denotes the single centre expansion coefficients for the orbital i/ϵ . The index i refers to the i th bound orbital, while ϵ refers to a continuum orbital with energy ϵ . Since CO is a linear molecule, it has rotational symmetry and hence only one m value is involved in the summation in eq. (1). For a heteronuclear molecule, like CO, the wavefunctions have no gerade or ungerade symmetry and therefore both even and odd values of l have to be included in eq. (1). This is unlike a homonuclear molecule, like N_2 , where only odd or even values of l are included in the summation in eq. (1) depending on whether the wavefunction has gerade or ungerade symmetry.

The continuum wavefunctions, ψ_ϵ , are calculated by solving the following Hartree-

Fock equations [23, 24, 27]:

$$\begin{aligned}
 & \underbrace{-\frac{1}{2}\nabla^2\psi_\epsilon(\mathbf{r})}_{\text{Kinetic energy}} + \underbrace{\sum_n^{nuc.} \frac{-Z_n}{|\mathbf{r}-\mathbf{R}_n|}\psi_\epsilon(\mathbf{r})}_{\text{Electron-nuclei}} + \underbrace{\sum_i^{orb.} a_i \int d\mathbf{r}p \frac{\psi_i^*(\mathbf{r}p)\psi_i(\mathbf{r}p)}{|\mathbf{r}-\mathbf{r}p|}\psi_\epsilon(\mathbf{r})}_{\text{Direct interaction}} \\
 & \quad - \underbrace{\sum_i^{orb.} b_i \int d\mathbf{r}p \frac{\psi_i^*(\mathbf{r}p)\psi_\epsilon(\mathbf{r}p)}{|\mathbf{r}-\mathbf{r}p|}\psi_i(\mathbf{r})}_{\text{Exchange interaction}} = \epsilon\psi_\epsilon(\mathbf{r}), \quad (2)
 \end{aligned}$$

where ψ_i is the wavefunction of the i th bound molecular orbital, a_i is the occupation of orbital i and b_i is a coefficient associated with the i th orbital, whose values are determined by the symmetry of the state. For more details, see our previous work [23]. \mathbf{R}_n and Z_n are the position with respect to the centre of mass, and the charge of nucleus n , respectively. In order to compute the continuum orbitals ψ_ϵ , we substitute ψ_ϵ and ψ_i using eq. (1) and use the non-iterative method [23, 24] to solve for the P_{lm}^ϵ coefficients.

2.3. Photo-ionisation

The photoionisation cross-section for an electron transitioning from an initial molecular orbital ψ_i to a final continuum molecular orbital ψ_ϵ is given by [28]

$$\sigma_{i \rightarrow \epsilon} = \frac{4}{3}\alpha\pi^2\omega N_i \sum_{M=-1,0,1} |D_{i\epsilon}^M|^2. \quad (3)$$

The fine-structure constant is denoted by α , the photon energy by ω , the occupation number of orbital i by N_i and the magnetic quantum number of the photon by M . In the length gauge, using eq. (1), the matrix element $D_{i\epsilon}^M$ is given by

$$\begin{aligned}
 D_{i\epsilon}^M &= \sqrt{\frac{4\pi}{3}} \sum_{lm,l'm'} \int_0^\infty dr P_{lm}^{i*}(r) r P_{l'm'}^\epsilon(r) \times \int d\Omega Y_{lm}^*(\theta, \phi) Y_{l'm'}(\theta, \phi) Y_{1M}(\theta, \phi) \quad (4) \\
 &= \sum_{lm,l'm'} (-1)^m \sqrt{(2l+1)(2l'+1)} \begin{pmatrix} l & l' & 1 \\ 0 & 0 & 0 \end{pmatrix} \begin{pmatrix} l & l' & 1 \\ -m & m' & M \end{pmatrix} \int_0^\infty dr P_{lm}^{i*}(r) r P_{l'm'}^\epsilon(r).
 \end{aligned}$$

Eq.(4) clearly shows that, by adapting the SCE for the bound and continuum wavefunctions, we significantly simplify the computation of the cross-section. Namely, the result of the angular integrals is expressed in terms of the Wigner-3j symbols [29] and we only have to solve a 1D integral numerically, which involves the single-centre expansion coefficients, $P_{lm}^{i/\epsilon}$. The computation of the matrix element $D_{i\epsilon}^M$ is more intensive for the heteronuclear molecule, CO, than the homonuclear N_2 as it involves both odd and even values for the l and l' numbers.

2.4. Auger decay

Auger decay rates have been calculated with a variety of different methods in existing work [30–40]. The general expression for the Auger rate, Γ , is given by [41]:

$$\Gamma = \overline{\sum} 2\pi |\mathcal{M}|^2 \equiv \overline{\sum} 2\pi |\langle \Psi_{fin} | H_I | \Psi_{init} \rangle|^2, \quad (5)$$

where $\overline{\sum}$ denotes a summation over the final states and an average over the initial states. $|\Psi_{init}\rangle$ and $|\Psi_{fin}\rangle$ are the wavefunctions of all electrons in the initial and final molecular state, respectively. H_I is the interaction Hamiltonian. In the m_a, m_b, S, M_S scheme, the Auger rate is given by [23]

$$\Gamma_{b,a \rightarrow s, \zeta} = \sum_{\substack{m_a m_b m_s m_\zeta \\ S M_S S' M'_S}} \pi N_{ab} N_h \sum_L |\mathcal{M}|^2, \quad (6)$$

with N_h being the number of holes in the orbital to be filled. a, b refer to the valence orbitals, s to the core orbital which is filled in and ζ refers to the continuum orbitals. S and M_S are the total spin and its orientation before the transition and S' and M'_S are the total spin and its orientation afterwards. As the CO orbitals have well-defined m , the summations over m will take only a single value. N_{ab} is the weighting factor related to the occupation of the valence orbitals which fill the hole given by

$$N_{ab} = \begin{cases} \frac{N_a N_b}{2 \times 2} & \text{for different orbitals} \\ \frac{N_a (N_a - 1)}{2 \times 2 \times 1} & \text{for same orbital.} \end{cases} \quad (7)$$

Here, N_a and N_b are the occupations of orbitals a and b , respectively. The matrix element, \mathcal{M} , is given by

$$\begin{aligned} \mathcal{M} = & \delta_S^{S'} \delta_{M_S}^{M'_S} \sqrt{(2l_s + 1)(2l_a + 1)(2l_\zeta + 1)(2l_b + 1)} \quad (8) \\ & \times \left[\sum_{\substack{kl_\zeta l_s \\ l_b l_a}} \sum_{q=-k}^k (-1)^{m_s+q+m_\zeta} \int dr_1 \int dr_2 P_{l_\zeta m_\zeta}^{\zeta*}(r_1) P_{l_s m_s}^{s*}(r_2) \frac{r_1^k}{r_2^{k+1}} P_{l_b m_b}^b(r_1) P_{l_a m_a}^a(r_2) \right. \\ & \times \begin{pmatrix} l_s & k & l_a \\ 0 & 0 & 0 \end{pmatrix} \begin{pmatrix} l_s & k & l_a \\ -m_s & q & m_a \end{pmatrix} \begin{pmatrix} k & l_\zeta & l_b \\ 0 & 0 & 0 \end{pmatrix} \begin{pmatrix} k & l_\zeta & l_b \\ -q & -m_\zeta & m_b \end{pmatrix} \\ & + (-1)^S \sum_{\substack{kl_\zeta l_s \\ l_b l_a}} \sum_{q=-k}^k (-1)^{m_s+q+m_\zeta} \int dr_1 \int dr_2 P_{l_\zeta m_\zeta}^{\zeta*}(r_1) P_{l_s m_s}^{s*}(r_2) \frac{r_1^k}{r_2^{k+1}} P_{l_a m_a}^a(r_1) P_{l_b m_b}^b(r_2) \\ & \left. \times \begin{pmatrix} l_s & k & l_b \\ 0 & 0 & 0 \end{pmatrix} \begin{pmatrix} l_s & k & l_b \\ -m_s & q & m_b \end{pmatrix} \begin{pmatrix} k & l_\zeta & l_a \\ 0 & 0 & 0 \end{pmatrix} \begin{pmatrix} k & l_\zeta & l_a \\ -q & -m_\zeta & m_a \end{pmatrix} \right] \end{aligned}$$

where $r_< = \min(r_1, r_2)$ and $r_> = \max(r_1, r_2)$. Due to rotational symmetry, each orbital has a single well-defined m number. This calculation is more computationally intensive in the heteronuclear case than in the homonuclear case, as the wavefunctions do not have gerade or ungerade symmetry and therefore will involve both odd and even values of l .

2.5. Dissociation

We treat the dissociation of the molecule phenomenologically, with rates based on FEL experiments with N_2 [20, 42]. This approximation is justified by the similarity between CO and N_2 , particularly with respect to their dissociative transitions [43]. The molecular ion CO^{2+} is treated as dissociating with a lifetime of 100 fs [42]. The final products of this dissociation, according to the experimental work in ref. [44], are C^+ and O^+ with 85% probability, C^{2+} and O with 9% probability, and C and O^{2+} with 6% probability. States of CO^{3+} without core holes are treated as instantaneously dissociating to C^+ and O^{2+} or C^{2+} and O^+ with equal probability, as is the case for N_2 [20, 23]. All states of CO^{4+} are treated as dissociating instantaneously to C^{2+} and O^{2+} [20, 23]. To determine how missing molecular orbitals just before dissociation map to missing atomic orbitals just after dissociation, we calculate overlaps between molecular and atomic orbitals. Specifically, we calculate the overlap $\langle \psi_a^{CO} | \psi_\alpha^{C/O} \rangle$ of each molecular orbital of neutral CO with each atomic orbital of neutral C and O, where a corresponds to a molecular orbital and α to an atomic orbital. We find that $\langle \psi_{1\sigma}^{CO} | \psi_{1s}^C \rangle \approx 1$, which means that the 1σ CO orbital with energy 542 eV corresponds to a $1s$ O orbital with energy 544 eV. Moreover, we find $\langle \psi_{2\sigma}^{CO} | \psi_{1s}^O \rangle \approx 1$, which means that the 2σ CO orbital with energy 296 eV corresponds to a $1s$ C orbital with energy 297 eV. The other molecular orbitals have overlaps with atomic orbitals on both atomic sites. In what follows, we use these overlaps to determine the possible dissociation products and the dissociation rates to different sets of atomic states. For example, for a CO^{2+} state with missing electrons in molecular orbitals a and b , the dissociation rate to atomic states missing electrons in atomic orbitals α and β is given by:

$$\Gamma_{a,b \rightarrow \alpha, \beta}^{C^{2+}+O} = 0.09 \times \Gamma_{a,b}^{CO^{2+}} \frac{|\langle \psi_a^{CO} | \psi_\alpha^C \rangle|^2 |\langle \psi_b^{CO} | \psi_\beta^C \rangle|^2}{\sum_{i,j} |\langle \psi_a^{CO} | \psi_i^C \rangle|^2 |\langle \psi_b^{CO} | \psi_j^C \rangle|^2} \quad (9)$$

$$\Gamma_{a,b \rightarrow \alpha, \beta}^{C^++O^+} = 0.85 \times \Gamma_{a,b}^{CO^{2+}} \frac{|\langle \psi_a^{CO} | \psi_\alpha^C \rangle|^2 |\langle \psi_b^{CO} | \psi_\beta^O \rangle|^2}{\sum_{i,j} |\langle \psi_a^{CO} | \psi_i^C \rangle|^2 |\langle \psi_b^{CO} | \psi_j^O \rangle|^2} \quad (10)$$

$$\Gamma_{a,b \rightarrow \alpha, \beta}^{C+O^{2+}} = 0.06 \times \Gamma_{a,b}^{CO^{2+}} \frac{|\langle \psi_a^{CO} | \psi_\alpha^O \rangle|^2 |\langle \psi_b^{CO} | \psi_\beta^O \rangle|^2}{\sum_{i,j} |\langle \psi_a^{CO} | \psi_i^O \rangle|^2 |\langle \psi_b^{CO} | \psi_j^O \rangle|^2}, \quad (11)$$

where $\Gamma_{a,b}^{CO^{2+}}$ is the rate of dissociation of molecular ion CO^{2+} with electrons missing from molecular orbitals a and b . This rate corresponds to a lifetime of 100 fs [42]. Note,

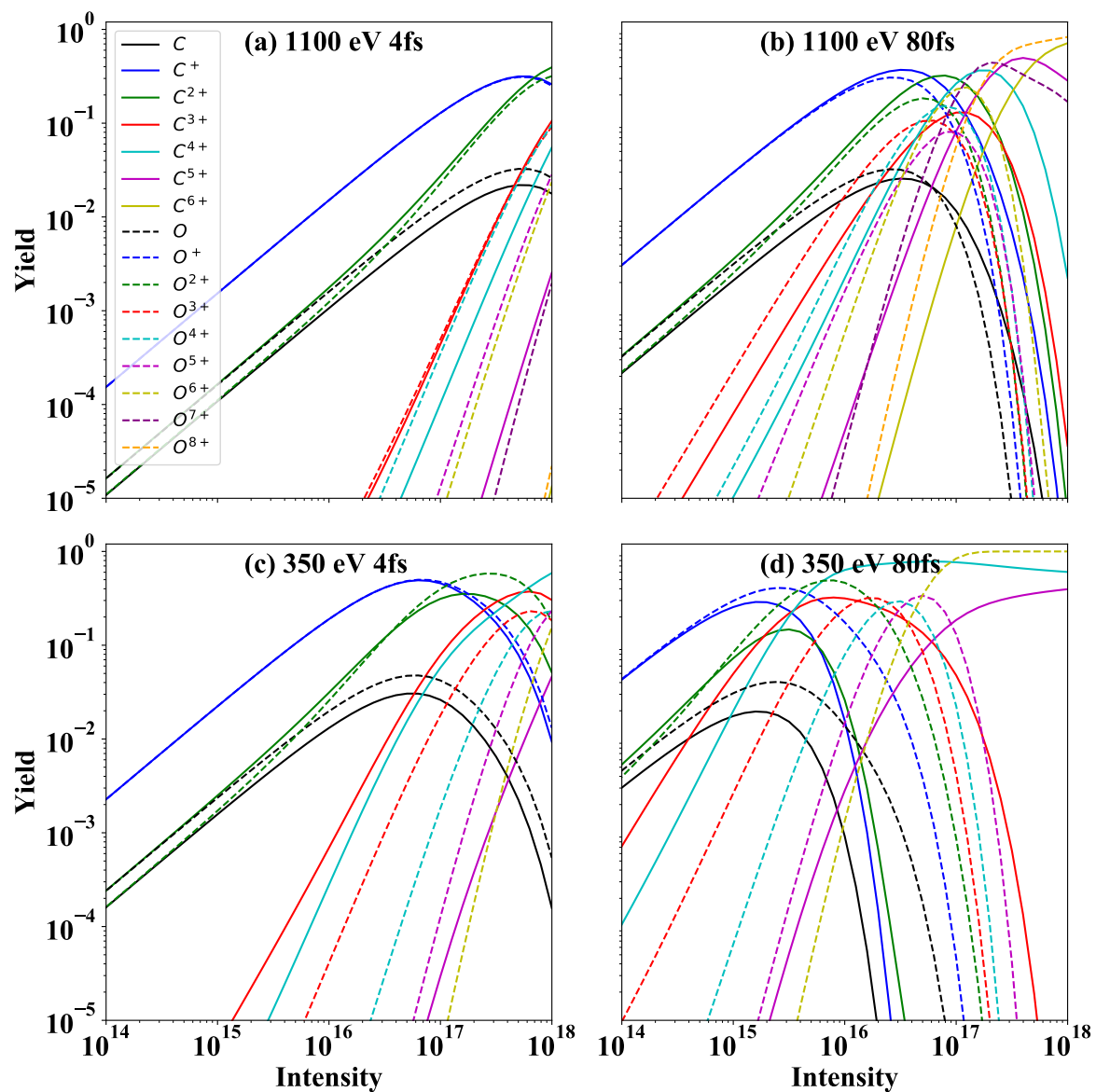


Figure 1. Carbon and oxygen ion yields, as a function of intensity, produced by CO interacting with FEL pulses with (a) 1100 eV and 4 fs FWHM (b) 1100 eV and 80 fs FWHM (c) 350 eV and 4 fs FWHM (d) 350 eV and 80 fs FWHM.

in eqs. 9-11, we only consider transitions to atomic ions with electrons missing from orbitals α and β if the relevant overlaps have values greater than 0.02.

3. Results

3.1. Ion Yields

3.1.1. Ion yield dependence on FEL pulse parameters In what follows, we identify how the C and O ion yields depend on different FEL pulses interacting with CO. In Fig. 1, we show the atomic ion yields of C and O produced by FEL pulses interacting with CO.

These ion yields are obtained as a function of intensity for FEL pulses of photon energy 1100 eV and pulse duration 4 fs Fig. 1(a) and 80 fs Fig. 1(b) as well as of photon energy 350 eV and pulse duration 4 fs Fig. 1(c) and 80 fs Fig. 1(d). The photon energy 1100 eV is sufficient to ionise an electron from the 1σ orbital, the innermost orbital of CO, while 350 eV allows for an electron to be removed from the 2σ orbital. Therefore, the photon energy of 350 eV does not allow for an electron to be removed from the O site of CO. An 80 fs duration FEL pulse allows for more photoionisations transitions to take place compared to a 4 fs duration pulse.

At a given intensity, for 1100 eV photon energy, comparing Fig. 1(a) with Fig. 1(b) and for 350 eV photon energy, comparing Fig. 1(c) with Fig. 1(d), we find that as expected the longer 80 fs pulse results in larger yields for the higher-charged states compared to the shorter 4 fs pulse. This is due to a larger number of photons being absorbed during the longer duration pulse. Moreover, we identify the effect of the photon energy, for a given pulse duration, by comparing the ion yields of the 350 eV pulses with the ion yields of the 1100 eV pulses. That is, we compare Fig. 1(a) with Fig. 1(c) and Fig. 1(b) with Fig. 1(d). We find that, at a given intensity, the ion yields for the higher-charged states are larger at a given intensity for the smaller 350 eV photon energy pulse. This is attributed to two factors. For a given intensity, a lower photon energy corresponds to a higher photon flux. In addition, the photoionisation cross-sections are higher for the lower 350 eV photon energy compared to the higher 1100 eV photon energy, resulting in more photoionisation processes.

3.1.2. C versus O atomic ion yields For a given charge state, the C and O atomic ion yields as a function of intensity are generally different, see Fig. 1. For both 1100 eV and 350 eV photon energies and 4 fs and 80 fs pulse durations, we compare C with O, C^+ with O^+ and C^{2+} with O^{2+} . We find these ion yields to be similar, since they are created mostly by the dissociation of CO^{2+} . Specifically, C^+ and O^+ are created in equal amounts, see eq. (10). For small intensities, the atomic ion C^{2+} has a slightly higher ion yield than O^{2+} , since C^{2+} is produced with a dissociation rate of $0.09 \times \Gamma_{a,b}^{CO^{2+}}$ (eq. (9)), while O^{2+} is produced with a rate of $0.06 \times \Gamma_{a,b}^{CO^{2+}}$ (eq. (11)). For higher intensities, the biggest difference between C^{2+} and O^{2+} ion yields, occurs for pulse parameters 350 eV photon energy and 80 fs pulse duration. The reason is that significantly more atomic photoionisation transitions after dissociation lead to the formation of O^{2+} compared to C^{2+} . This is shown in Fig. 2(d). Note, in Fig. 2(a-d), we plot, as a function of intensity, the average number of atomic single-photon ionisation transitions that lead to the formation of each atomic ion state.

We now focus on the higher-charged states C^{n+} and O^{n+} , where $n = 3, 4, 5$. At a given intensity, we find that for the 1100 eV photon energy, both for the 4 fs and 80 fs pulses, the yield of the O^{n+} ion is higher than the yield of the C^{n+} ion. The reason is that the single-photon ionisation cross-section to remove an electron from the 1σ molecular orbital or from the $1s$ orbital in oxygen is higher than the cross-section to remove an electron from the 2σ molecular orbital or from the $1s$ orbital in carbon. Fig. 2(a) and

Fig. 2(b) show that atomic photoionisation transitions play a more important role for the formation of C^{5+} and O^{5+} , roughly two transitions, compared to one or less atomic transitions leading to the formation of C^{n+} and O^{n+} with $n = 3, 4$. At a given intensity, we find that for the 350 eV photon energy, both for the 4 fs and 80 fs pulses, the yield of the C^{n+} ion is higher than the yield of the O^{n+} ion where $n = 3$ or 4. The reason is that a photon energy of 350 eV is insufficient to ionise a core electron corresponding to the oxygen atomic site in CO or to ionise a 1s electron from an oxygen atomic ion. Hence, while C^{4+} is formed by an inner-shell atomic photoionisation from C^{2+} followed by an Auger process, O^{4+} is formed by two valence atomic photoionisation transitions from O^{2+} . Indeed, comparing Fig. 2(c-d) with Fig. 2(a-b), we find that the number of atomic transitions to form C^{4+} remains roughly equal to one both for 1100 eV and 350 eV. However, for O^{4+} the number of photoionisations increases to two in the 350 eV case compared to one in the 1100 eV case. Finally, for the 350 eV case, C^{5+} and O^{5+} are both created by three valence atomic photoionisation transitions, resulting in similar ion yields.

3.1.3. Comparison of C, O and N atomic ion yields Next, we compare the N atomic ion yields produced by the interaction of N_2 with an FEL pulse with the C and O atomic ion yields produced when the same FEL pulse interacts with CO. Specifically, we compare the N, C and O atomic ion yields for an FEL pulse of 1100 eV photon energy and duration 4 fs Fig. 3(a) and 80 fs Fig. 3(b). Fig. 3(a) and Fig. 3(b) clearly show that, at a given intensity, each N ion yields is larger than the respective C and O ion yields. This is due to the cross-sections of photoionisation transitions in N_2 being higher than the cross-section for photoionisation transitions in CO. Indeed, in N_2 the core orbitals $1\sigma_g$ and $1\sigma_u$ have very similar ionisation energies, roughly equal to 680 eV, and large photoionisation cross-sections approximately equal to 0.0023 a.u. for photon energy of 1100 eV. However, in CO, the ionisation energy of the core orbital 1σ , 544 eV, is significantly higher than the ionisation energy of the 2σ , 296 eV. As a result, the photoionisation cross-section from the 1σ orbital (0.0018 a.u.) in CO is significantly higher than the photoionisation cross-section from the 2σ orbital (0.00077 a.u.).

3.2. DCH contributions

We are interested in the proportion of each atomic ion yield that is reached by accessing various types of double-core-hole (DCH) states. We calculate these proportions by using an expanded set of rate equations. That is, for each electronic configuration, we consider four equations, which keep track of the population that reaches this state after accessing a TSDCH state, after accessing a SSDCH state, on the C or on the O site respectively, as well as the population which does not access a DCH state. The proportions of each atomic ion yield that are formed via accessing different DCH states are shown in Fig. 4 for a 4 fs pulse duration with intensity of $10^{18} Wcm^{-2}$. We choose these pulse parameters as they favour the production of DCH states. Indeed, FEL pulses of short duration and

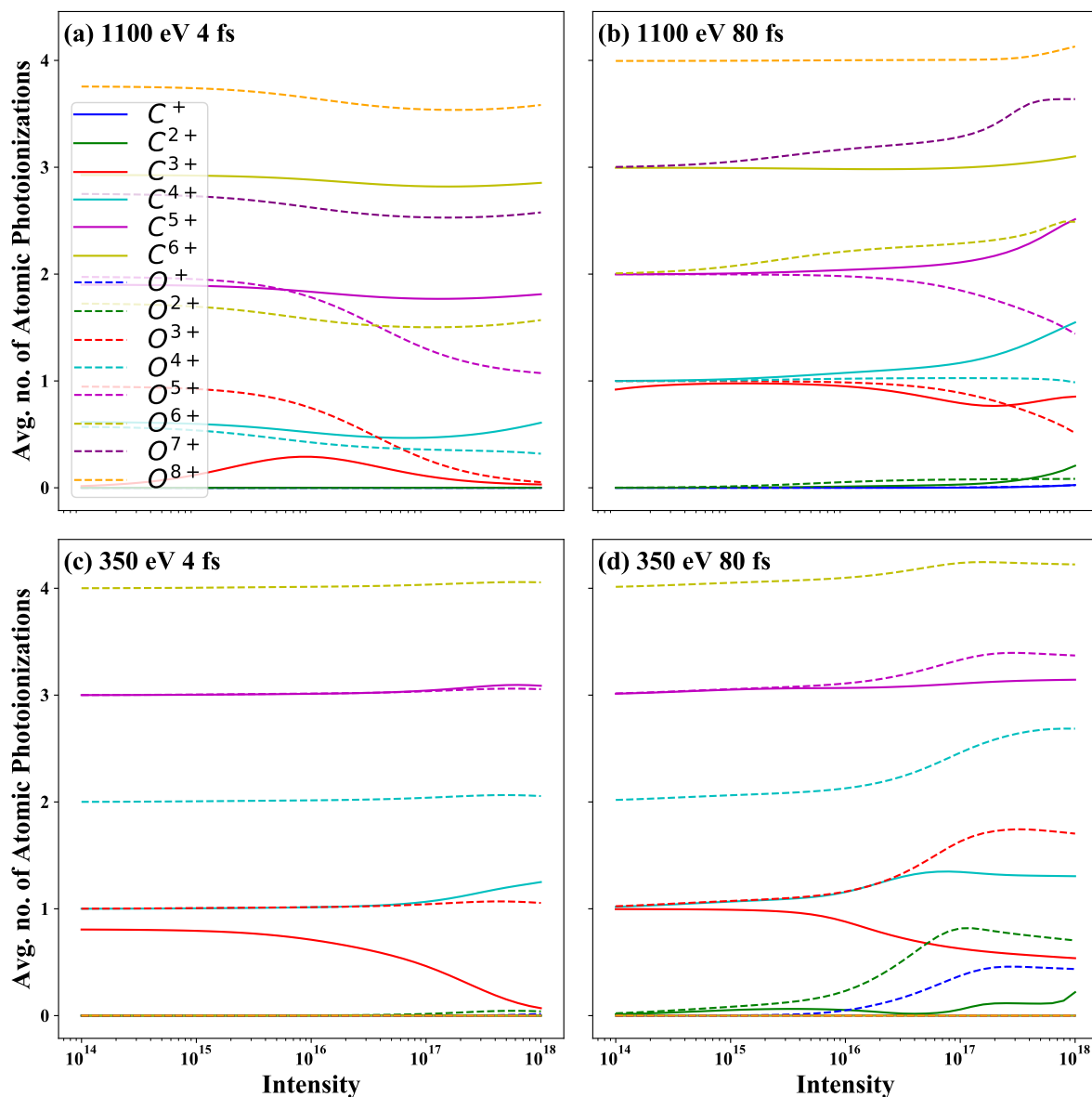


Figure 2. Average number of atomic single-photon ionisations, as a function of intensity, for each charged ion produced by CO interacting with FEL pulses with (a) 1100 eV and 4 fs FWHM (b) 1100 eV and 80 fs FWHM (c) 350 eV and 4 fs FWHM (d) 350 eV and 80 fs FWHM.

high intensity favour more single-photon ionisation transitions occurring in a certain time interval compared to longer and lower intensity FEL pulses. Moreover, in addition to the 1100 eV photon energy used in our calculations in the previous sections, we also consider a photon energy of 700 eV. The reason is that 700 eV is sufficient to photoionise both the 1σ and 2σ molecular orbitals in CO, as well as the $1\sigma_g$ and $1\sigma_u$ orbitals in N_2 and at the same time these cross-sections are higher than for the 1100 eV case.

Examining Fig. 4, we see that the proportion of the ion yields which accesses a DCH generally increases at higher-charged ion yields. This is expected as transition pathways which involve a pair of two core photoionisations typically lead to higher-charged ions.

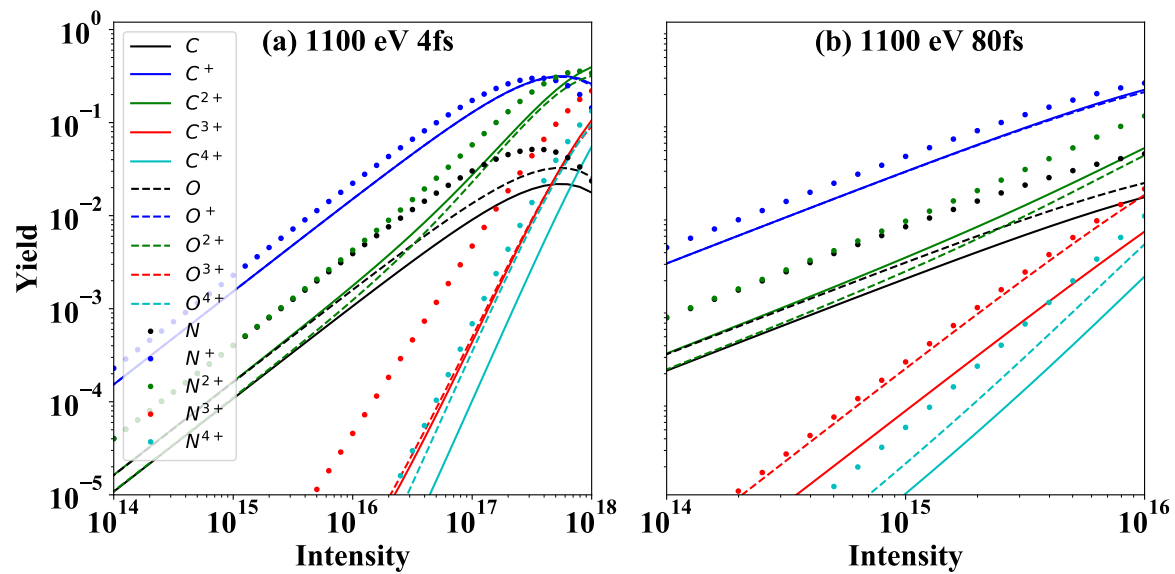


Figure 3. Carbon and oxygen ion yields, as a function of intensity, produced by CO interacting with an FEL pulse of 1100 eV photon energy and 4 fs (a) and 80 fs (b) FWHM contrasted with nitrogen ion yields produced by N₂ interacting the same pulses.

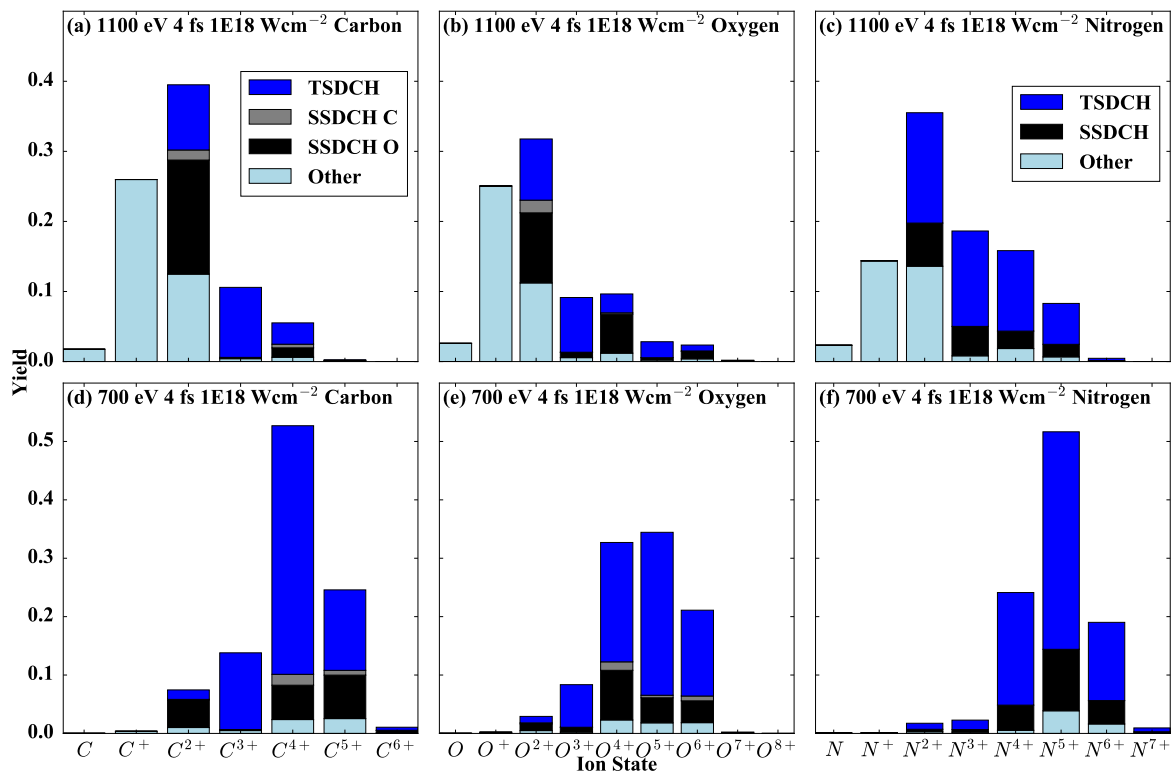


Figure 4. Atomic ion yields produced by FEL pulses with 1100 eV or 700 eV photon energy, 4 fs FWHM and 10^{18} Wcm⁻² intensity interacting with CO ((a), (b), (d) and (e)) or N₂ ((c) and (f)). For each ion yield, we show the proportion of this ion yield that is reached by accessing a certain type of double-core-hole state.

For this high-intensity and short-duration FEL pulse the C and O ions with charges 2,3 and 4 are mainly produced by the dissociation of CO^{4+} . We find that almost all of the C^{3+} and O^{3+} ion yields are produced via pathways involving TSDCH states. The reason is that after dissociation of CO^{4+} to C^{2+} and O^{2+} , each doubly-charged ion is created with a core hole. Each core hole is then filled in by an Auger decay leading to the production of C^{3+} and O^{3+} . A large proportion of the O^{4+} yield accesses a SSDCH state with the core holes localised on the oxygen. Regarding the O^{4+} ion, it is formed by dissociation of CO^{4+} to O^{2+} with two $1s$ core holes, which are then filled in by two Auger transitions. Hence, O^{4+} is mostly formed by accessing a SSDCH state of CO. In addition, we find that C^{2+} and O^{2+} are formed after the dissociation of CO^{4+} with no core holes. However, CO^{4+} before dissociation, accesses mostly SSDCH states on the oxygen side. This is due to the much higher photoionisation cross-section to transition from the 1σ orbital compared to transitioning from the 2σ orbital.

Comparing Fig. 4(d) with Fig. 4(a) and Fig. 4(e) with Fig. 4(b), we find that, for the 700 eV case, higher-charged ion states are produced with a higher proportion of these ion states accessing a TSDCH state. This is in accord with higher photoionisation cross-sections from both the 1σ and 2σ molecular orbitals for 700 eV photon energy, compared to 1100 eV. Finally, comparing the N ion yields in Fig. 4(c) with the C and O ion yields in Fig. 4(a) and Fig. 4(b) for 1100 eV and the N ion yields in Fig. 4(f) with the C and O ion yields in Fig. 4(d) and Fig. 4(e) for 700 eV, we find that N_2 dissociates into higher-charged ion states. Moreover, we find that a higher proportion of each of these N higher-charged ion states accesses a TSDCH state. This is due to the higher photoionisation cross-sections of the N_2 core orbitals, particularly the $1\sigma_u$ cross-section, which is much higher than the 2σ cross-section of CO.

4. Conclusions

In this work, we have investigated the interaction of FEL pulses with CO, a heteronuclear diatomic molecule. In particular, we have calculated the atomic ion yields produced when neutral CO is exposed to a variety of different FEL pulses. We identify higher yields for oxygen ion states for charges 3, 4 and 5, compared to carbon. We also find this to be the case for a photon energy of 1100 eV, which is sufficient to ionise the 1σ molecular orbital corresponding to the $1s$ core hole on the O site. However, for a photon energy of 350 eV, which does not access the 1σ molecular orbital, we find that the higher-charged C atomic ions are favoured over the O ions. Finally, we find that high-intensity short-duration laser pulses, with a photon energy sufficient to ionise both core orbitals in CO, favour the production of higher-charged states that are mainly formed by accessing TSDCH states.

Acknowledgments. A.E. and H. I. B. Banks acknowledge the use of the Legion computational resources at UCL. This work was funded by the Leverhulme Trust Research Project Grant 2017-376.

References

- [1] Pellegrini C 2012 *Eur. Phys. J. H* **37** 659–708
- [2] Bostedt C, Bozek J, Bucksbaum P H, Coffee R, B Hastings J, Huang Z, Lee R, Schorb S, Corlett J N, Denes P, Emma P, Falcone R, Schoenlein R W, Doumy G, Kanter E, Kraessig B, Southworth S, Young L, Fang L, Hoener M, Berrah N, Roedig C and DiMauro L 2013 *J. Phys. B: At., Mol. Opt. Phys.* **46** 164003
- [3] Emma P, Akre R, Arthur J, Bionta R, Bostedt C, Bozek J, Brachmann A, Bucksbaum P, Coffee R, Decker F, Ding Y, Dowell D, Edstrom S, Fisher A, Frisch J, Gilevich S, Hastings J, Hays G, Hering P, Huang Z, Iverson R, Loos H, Messerschmidt M, Miahnahri A, Moeller S, Nuhn H, Pile G, Ratner D, Rzepiela J, Schultz D, Smith T, Stefan P, Tompkins H, Turner J, Welch J, White W, Wu J, Yocky G and Galayda J 2010 *Nat. Photonics* **4** 641–647 ISSN 1749-4885
- [4] Marangos J P 2011 *Contemp. Phys.* **52** 551–569 <http://dx.doi.org/10.1080/00107514.2011.607290>
- [5] Ullrich J, Rudenko A and Moshhammer R 2012 *Annu. Rev. Phys. Chem.* **63** 635–660 <http://dx.doi.org/10.1146/annurev-physchem-032511-143720>
- [6] Schlichting I and Miao J 2012 *Curr. Opin. Struct. Biol.* **22** 613 – 626 ISSN 0959-440X <http://www.sciencedirect.com/science/article/pii/S0959440X12001261>
- [7] Neutze R, Wouts R, van der Spoel D, Weckert E and Hajdu J 2000 *Nature* **406**(6797) 752–757
- [8] Redecke L, Nass K, DePonte D P, White T A, Rehders D, Barty A, Stellato F, Liang M, Barends T R, Boutet S, Williams G J, Messerschmidt M, Seibert M M, Aquila A, Arnlund D, Bajt S, Barth T, Bogan M J, Caleman C, Chao T C, Doak R B, Fleckenstein H, Frank M, Fromme R, Galli L, Grotjohann I, Hunter M S, Johansson L C, Kassemeyer S, Katona G, Kirian R A, Koopmann R, Kupitz C, Lomb L, Martin A V, Mogk S, Neutze R, Shoeman R L, Steinbrener J, Timneanu N, Wang D, Weierstall U, Zatsepin N A, Spence J C H, Fromme P, Schlichting I, Duszynski M, Betzel C and Chapman H N 2013 *Science* **339** 227–230 ISSN 0036-8075 <http://science.sciencemag.org/content/339/6116/227>
- [9] Cederbaum L S, Tarantelli F, Sgamellotti A and Schirmer J 1986 *J. Chem. Phys.* **85** 6513–6523 <http://dx.doi.org/10.1063/1.451432>
- [10] Cederbaum L S, Tarantelli F, Sgamellotti A and Schirmer J 1987 *J. Chem. Phys.* **86** 2168–2175 <https://doi.org/10.1063/1.452756>
- [11] Tashiro M, Ehara M, Fukuzawa H, Ueda K, Buth C, Kryzhevoi N V and Cederbaum L S 2010 *J. Chem. Phys.* **132** 184302 <http://dx.doi.org/10.1063/1.3408251>
- [12] Salén P, van der Meulen P, Schmidt H T, Thomas R D, Larsson M, Feifel R, Piancastelli M N, Fang L, Murphy B, Osipov T, Berrah N, Kukk E, Ueda K, Bozek J D, Bostedt C, Wada S, Richter R, Feyer V and Prince K C 2012 *Phys. Rev. Lett.* **108**(15) 153003 <https://link.aps.org/doi/10.1103/PhysRevLett.108.153003>

- [13] Piancastelli M N 2013 *Eur. Phys. J. Spec. Top.* **222** 2035–2055 <https://doi.org/10.1140/epjst/e2013-01985-9>
- [14] Berrah N, Fang L, Murphy B, Osipov T, Ueda K, Kukk E, Feifel R, van der Meulen P, Salen P, Schmidt H T, Thomas R D, Larsson M, Richter R, Prince K C, Bozek J D, Bostedt C, Wada S i, Piancastelli M N, Tashiro M and Ehara M 2011 *Proceedings of the National Academy of Sciences* **108** 16912–16915 <http://www.pnas.org/content/108/41/16912.abstract>
- [15] Santra R, Kryzhevoi N V and Cederbaum L S 2009 *Phys. Rev. Lett.* **103**(1) 013002 <https://link.aps.org/doi/10.1103/PhysRevLett.103.013002>
- [16] Fang L, Hoener M, Gessner O, Tarantelli F, Pratt S T, Kornilov O, Buth C, Gühr M, Kanter E P, Bostedt C, Bozek J D, Bucksbaum P H, Chen M, Coffee R, Cryan J, Glowonia M, Kukk E, Leone S R and Berrah N 2010 *Phys. Rev. Lett.* **105**(8) 083005 <http://link.aps.org/doi/10.1103/PhysRevLett.105.083005>
- [17] Fang L, Osipov T, Murphy B, Tarantelli F, Kukk E, Cryan J P, Glowonia M, Bucksbaum P H, Coffee R N, Chen M, Buth C and Berrah N 2012 *Phys. Rev. Lett.* **109**(26) 263001 <https://link.aps.org/doi/10.1103/PhysRevLett.109.263001>
- [18] Zhaunerchyk V, Kamińska M, Mucke M, Squibb R J, Eland J H D, Piancastelli M N, Frasinski L J, Grilj J, Koch M, McFarland B K, Sistrunk E, Gühr M, Coffee R N, Bostedt C, Bozek J D, Salén P, v d Meulen P, Linusson P, Thomas R D, Larsson M, Foucar L, Ullrich J, Motomura K, Mondal S, Ueda K, Richter R, Prince K C, Takahashi O, Osipov T, Fang L, Murphy B F, Berrah N and Feifel R 2015 *J. Phys. B: At., Mol. Opt. Phys.* **48** 244003 <http://stacks.iop.org/0953-4075/48/i=24/a=244003>
- [19] Buth C, Liu J C, Chen M H, Cryan J P, Fang L, Glowonia J M, Hoener M, Coffee R N and Berrah N 2012 *J. Chem. Phys.* **136** 214310 <http://dx.doi.org/10.1063/1.4722756>
- [20] Liu J C, Berrah N, Cederbaum L S, Cryan J P, Glowonia J M, Schafer K J and Buth C 2016 *J. Phys. B: At., Mol. Opt. Phys.* **49** 075602 <http://stacks.iop.org/0953-4075/49/i=7/a=075602>
- [21] Hill J R, Tokmakoff A, Peterson K A, Sauter B, Zimdars D, Dlott D D and Fayer M D 1994 *J. Phys. Chem.* **98** 11213–11219 <https://doi.org/10.1021/j100094a032>
- [22] Levantino M, Schirò G, Lemke H T, Cottone G, Glowonia J M, Zhu D, Chollet M, Ihee H, Cupane A and Cammarata M 2015 *Nat. Commun.* **6** 6772 <https://doi.org/10.1038/ncomms7772>
- [23] Banks H I B, Little D A, Tennyson J and Emmanouilidou A 2017 *Phys. Chem. Chem. Phys.* **19**(30) 19794–19806 <http://dx.doi.org/10.1039/C7CP02345F>
- [24] Demekhin P V, Ehresmann A and Sukhorukov V L 2011 *J. Chem. Phys.* **134** 024113

- [25] Werner H J, Knowles P J, Lindh R, Manby F R, Schütz M *et al.* 2010 MOLPRO, a package of ab initio programs see <http://www.molpro.net/>
- [26] Gilliam O R, Johnson C M and Gordy W 1950 *Phys. Rev.* **78**(2) 140–144 <https://link.aps.org/doi/10.1103/PhysRev.78.140>
- [27] Bransden B H and Joachain C J 2003 *Physics of Atoms and Molecules* (Pearson Education)
- [28] Sakurai J J 1994 *Modern Quantum Mechanics* (Addison-Wesley)
- [29] Shore B W and Menzel D H 1968 *Principles of Atomic Spectra* (Wiley)
- [30] Wallis A O G, Lodi L and Emmanouilidou A 2014 *Phys. Rev. A* **89**(6) 063417 <http://link.aps.org/doi/10.1103/PhysRevA.89.063417>
- [31] Bhalla C P, Folland N O and Hein M A 1973 *Phys. Rev. A* **8**(2) 649–657
- [32] Pulkkinen H, Aksela S, Sairanen O P, Hiltunen A and Aksela H 1996 *J. Phys. B: At., Mol. Opt. Phys.* **29** 3033 <http://stacks.iop.org/0953-4075/29/i=14/a=016>
- [33] Lablanquie P, Andric L, Palaudoux J, Becker U, Braune M, Viefhaus J, Eland J and Penent F 2007 *J. Electron Spectrosc. Relat. Phenom.* **156–158** 51 – 57 ISSN 0368-2048 [//www.sciencedirect.com/science/article/pii/S0368204806002106](http://www.sciencedirect.com/science/article/pii/S0368204806002106)
- [34] Son S K and Santra R 2012 *Phys. Rev. A* **85**(6) 063415 <http://link.aps.org/doi/10.1103/PhysRevA.85.063415>
- [35] Bolognesi P, Coreno M, Avaldi L, Storchi L and Tarantelli F 2006 *J. Chem. Phys.* **125** 054306 <http://dx.doi.org/10.1063/1.2213254>
- [36] Feyer V, Bolognesi P, Coreno M, Prince K C, Avaldi L, Storchi L and Tarantelli F 2005 *J. Chem. Phys.* **123** 224306 <http://dx.doi.org/10.1063/1.2137311>
- [37] Püttner R, Fukuzawa H, Liu X J, Semenov S K, Cherepkov N A, Tanaka T, Hoshino M, Tanaka H and Ueda K 2008 *J. Phys. B: At., Mol. Opt. Phys.* **41** 141001 <http://stacks.iop.org/0953-4075/41/i=14/a=141001>
- [38] Iwayama H, Sisourat N, Lablanquie P, Penent F, Palaudoux J, Andric L, Eland J H D, Bučar K, Žitnik M, Velkov Y, Hikosaka Y, Nakano M and Shigemasa E 2013 *J. Chem. Phys.* **138** 024306 <http://dx.doi.org/10.1063/1.4773294>
- [39] Storchi L, Tarantelli F, Veronesi S, Bolognesi P, Fainelli E and Avaldi L 2008 *J. Chem. Phys.* **129** 154309 <http://dx.doi.org/10.1063/1.2993317>
- [40] Griffiths W J, Correia N, Keane M P, de Brito A N, Svensson S and Karlsson L 1991 *J. Phys. B: At., Mol. Opt. Phys.* **24** 4187 <http://stacks.iop.org/0953-4075/24/i=19/a=014>
- [41] Pauli W 2000 *Wave Mechanics: Volume 5 of Pauli Lectures on Physics* (Wiley)
- [42] Beylerian C and Cornaggia C 2004 *J. Phys. B: At., Mol. Opt. Phys.* **37** L259 <http://stacks.iop.org/0953-4075/37/i=13/a=L02>

- [43] Gaire B, McKenna J, Johnson N G, Sayler A M, Parke E, Carnes K D and Ben-Itzhak I 2009 *Phys. Rev. A* **79**(6) 063414 <https://link.aps.org/doi/10.1103/PhysRevA.79.063414>
- [44] Hitchcock A, Lablanquie P, Morin P, E L, Simon M, Thiry P and Nenner I 1988 *Phys. Rev. A* **37** 2448–2466